Research Article/ Civil and Sanitary Engineering https://doi.org/10.15446/ing.investig.85937

Study of a Semi-Active Control System to Reduce Lateral Displacement in Framed Structures under Seismic Load

Estudio de un sistema de control semi-activo para reducir los desplazamientos laterales en estructuras aporticadas bajo cargas sísmicas

Luis A. Lara-Valencia[1] Yamile Valencia-González[2], and David M. Bedoya-Zambrano[3]

ABSTRACT

This study presents the numerical implementation of a semi-active control system used to reduce lateral displacements in framed structures under seismic loads. To manage forces in the structures, two controllable fluid devices called magnetorheological (MR) dampers were used together with a fuzzy logic (FL) algorithm to determine the optimal control forces. The FL controller was programmed based on a set of 49 inference rules using two input parameters: displacement and velocity of the first story of the uncontrolled structure. The voltage applied to the MR dampers was the output parameter of the control algorithm, thus altering the damping forces in the system. To evaluate the performance of the proposed controller, three plane frame structures with different geometric configurations were modeled and subjected to four different real ground acceleration records. The results obtained in this study show a considerable reduction in the displacement, acceleration, and inter-story drift for all the studied structures, demonstrating the effectiveness and efficiency of the controller at improving the damping characteristics in structures.

Keywords: magnetorheological dampers, structure control, earthquake load, reduction of lateral displacements

RESUMEN

Este estudio presenta el desarrollo numérico de un sistema de control semiactivo empleado para reducir los desplazamientos en estructuras aporticadas bajo cargas sísmicas. Para administrar las fuerzas en las estructuras se usaron dos dispositivos de fluido controlable llamados amortiguadores magnetoreológicos (MR) junto con un algoritmo de control basado en lógica difusa (FL), con el fin de determinar las fuerzas de control óptimas. El controlador FL fue programado con base en un conjunto de 49 reglas de inferencia, para las cuales se emplearon dos parámetros de entrada: desplazamiento y velocidad del primer piso de la estructura no controlada. El voltaje aplicado a los amortiguadores MR fue el parámetro de salida del algoritmo de control, modificando de esta manera las fuerzas de amortiguamiento del sistema. Para evaluar el desempeño del controlador propuesto, se modelaron tres pórticos planos con diferente configuración geométrica, sometiéndolos a cuatro registros reales y diferentes de aceleraciones del suelo. Los resultados obtenidos indican una considerable reducción en el desplazamiento, la aceleración y las derivas de entrepiso en todas las estructuras estudiadas, demostrando la eficacia y eficiencia del controlador para mejorar las características de amortiguamiento en estructuras.

Palabras clave: amortiguadores magnetoreológicos, control estructural, carga sísmica, reducción de desplazamientos laterales

Received: March 29th, 2020
Accepted: December 5th, 2021

Introduction

Structural control can be successful through different methodologies, among which is the modification of the structural system's stiffness, mass, shape, or damping (Housner *et al*., 1997; Kaveh *et al*., 2020; Shih and Sung, 2021). This can also be classified in up to four different control groups: active control (Bitaraf *et al*., 2012; Gutiérrez and Navarro, 2013; Kannan *et al*., 1995; Khodabandolehlou *et al*., 2018; Mohammadi *et al*., 2021; Pourzeynali *et al*., 2007; Smanchai and Yao, 1978), passive control (Arzeytoon *et al*., 2017; Basili and de Angelis, 2007; Chowdhury *et al*., 2021; Constantinou, 1994; Lara-Valencia *et al*., 2020; Selmani, 2020; Zhang and Balendra, 2013; Zhao *et al*., 2020), hybrid control (Kim and Adeli, 2005; Omidi and Mahmoodi, 2015; Subramaniam *et al*., 1996; Taniguchi *et al*., 2016; Yang *et al*., 1992; Zhou and Zheng, 2020), and semi-active control (Amini *et al*., 2015; Bathaei *et al*., 2018; Behrooz *et al*., 2014; Cha and Agrawal, 2017; K-Karamodin and H-Kazemi, 2010; Kori and Jangid, 2008; Madhekar and Jangid, 2009; Singh *et al*., 1997; Xu *et al*., 2003).

[1] Civil engineer, Universidad Nacional de Colombia, Colombia. Ph.D. in Structures and Civil Construction, Universidade de Brasilia, Brasil. Affiliation: Associate Professor, Universidad Nacional de Colombia, Medellín branch, Colombia. E-mail: lualarava@unal.edu.co

[2] Civil engineer, Universidad Nacional de Colombia, Colombia. Ph.D. in Geotechnical Engineering, Universidade de Brasilia, Brasil. Affiliation: Associate Professor, Universidad Nacional de Colombia, Medellín branch, Colombia. E-mail: yvalenc0@unal.edu.co

[3] Civil engineer, Universidad Nacional de Colombia, Colombia. Master's student in Structures, Universidad Nacional de Colombia, Medellín branch, Colombia. E-mail: dmbedoyaz@unal.edu.co

How to cite: Lara-Valencia, L., Valencia-González, Y., and Bedoya-Zambrano, D. (2022). Study of a Semi-Active Control System to Reduce Lateral Displacement in Framed Structures under Seismic Load. *Ingeniería e Investigación, 42*(3), e85937. https://doi.org/10.15446/ing.investig.85937

Today, semi-active controllers are probably the most popular family of structural control systems, which is mainly due to their potential to safeguard structural systems through sophisticated mechanisms, with the ability to operate and reduce the response of the monitored structures by using small portable external energy sources. This characteristic causes semi-active devices to show similar results to those of active control systems, due to the fact that the former devices use just a fraction of the energy required by the latter, which makes them safe, reliable, and ideal devices to face the great magnitude of natural hazards.

In the last decades, the study of semi-active controllers has been the focus of interest for many researchers, who have made various contributions to the development and refinement of control devices and algorithms in order to improve the performance of structures subjected to dynamic solicitations. In this way, devices such as controllable fluid dampers (Cruze *et al*., 2018; Cruze *et al*., 2021; Pahlavan and Rezaeepazhand, 2007), semi-active stiffness dampers (SASD)and semi-active tuned liquid column dampers (TLCD) (Kataria and Jangid, 2016), piezoelectric dampers (Zamani *et al*., 2017), friction variable dampers (Downey *et al*., 2016), and semi-active tuned mass dampers (Sun and Nagarajaiah, 2014) stand out as attractive alternatives to developing control systems to reduce lateral displacements in structures.

Magnetorheological dampers (MR dampers) are semi-active devices used for structural control. MR dampers and electrorheological dampers (ER dampers) are classified in the literature as controllable fluid dampers, mainly due to the special characteristics of the fluid that works in the tube of the absorber. MR dampers use magnetorheological fluid, which owes its name to the fact that micron-sized, magnetizable particles are randomly dispersed in an appropriate carrier liquid. Thus, when the fluid is exposed to a magnetic field, the magnetizable particles form parallel linear chains to the field, thus changing the fluid state, restricting the piston movement of the device, and increasing the flow resistance. This particularity allows magnetorheological dampers to develop variable non-linear damping forces, which depend on the voltage applied to the device, thus obtaining an energy dissipation mechanism with the potential to control the responses in real structural systems.

A numerical study to determine the structural behavior and performance of three plane frame buildings equipped with a semi-active control strategy based on MR dampers is carried out in this work. Four different ground motion earthquakes excite these buildings in order to analyze the potential use of this type of device. To this effect, a controller that uses two MR dampers governed by a fuzzy logic algorithm is used. This algorithm is responsible for managing the damping forces required by the structural system, so that the energy of the ground motion is rapidly and optimally dissipated, aiming at the reduction of the structure's response at all stories. A comparative analysis is also performed to compare the response of controlled and uncontrolled structural systems. It assesses the effectiveness of the controller used and its relevance in reducing the lateral displacement in the analyzed structures.

Methodology

Three different plane frame buildings have been discretized to set up the numerical model required to simulate the conditions of the controlled and uncontrolled systems. Each of these structures has been equipped with and without a control system based on MR dampers governed by a fuzzy logic algorithm (Lara-Valencia *et al*., 2015; Lara-Valencia, 2011; Liu *et al*., 2001; Wilson, 2005). To examine the effectiveness of the proposed controller, the uncontrolled and controlled configurations of the buildings are subjected to four different earthquake acceleration records. In this way, the results obtained allow comparing the behavior of each structure in its uncontrolled and controlled states in order to establish the impact of semi-active controllers in the reduction of lateral displacements.

The controlled structural systems are equipped with MR dampers partially based on the RD-1005-3 reference damper manufactured by the Lord Corporation (Lord Company, 2006). The location and number of devices used is the same in all the numerical models, prioritizing the installation of the MR dampers on the lower stories of the buildings. It should be noted that the performance of MR dampers is sensitive to the ground motion acting on the structure. The control system adapts according to the inputs (*i.e.*, the displacements and velocities of the structure), thus determining the optimal damping forces required to reduce the structural response.

The ground motion records used to excite the structures corresponds to the North-South component of El Centro earthquake, which occurred in United States in 1940; the ground motion known as Christchurch-Lyttelton that took place in New Zealand in 2011; the acceleration record of Mistrato in Colombia, which occurred in 1979; and the earthquake ground motion that occurred in Algarrobo, Chile in 1985.

Modeled structural systems

Three buildings discretized as plane frames were the structures chosen to be studied in this work, assuming the rigid diaphragm hypothesis as valid. Each developed model has the following dimensions: 2,8 m of floor-to-floor height and 6 m of column spacing. The maximum heights of the structural systems are 5,6, 22,4, and 30,8 m, which are related to buildings with two (model A), eight (model B), and eleven stories (model C), respectively. The two- and eight-floor buildings consist of a single span, while the eleven-floor building consists of four spans with variable heights. Concrete with a compressive strength (f'_c) of 28 MPa is assumed to be the material used for the construction of the frames. The sections of beams and columns are

assumed to be square, with cross-sectional areas of 30 and 40 cm, respectively. The fundamental frequencies of the structures are 36,32, 7,48, and 7,19 rad/sec for models A, B, and C, respectively. The damping matrix is calculated as a Rayleigh damping matrix proportional to the stiffness and mass matrices, assuming a critical damping ratio of 5% for the first and last modes of vibration. Figure 1 illustrates the frames used.

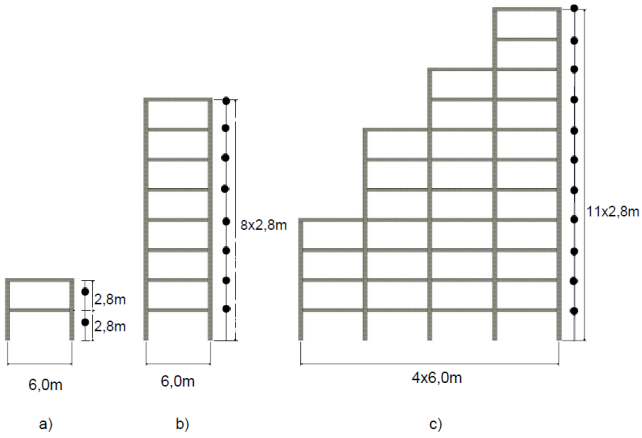

Figure 1. (a) Model A: two-floor building; (b) model B: eight-floor building; (c) model C: eleven-floor building
Source: Authors

MR dampers

The devices used to dissipate the energy generated in the structures as a consequence of the accelerations of the soil where buildings are founded are modified dissipators based on the MR damper type RD 1005-3 built by the Lord Corporation (Lord Company, 2006). This reference needs an adjustment to be able to reduce the response of the structures used in the numerical study. This adjustment consists of an increase in the damping forces generated by the device. In this way, the MR dampers produced damping forces of 2 224 N at factory settings. After modification, the device produces ten times more damping forces according to the scale of the modeled structures.

Two dampers were used for all the modeled buildings. The first one was installed on the first story and the second one on the second. The numerical model used to simulate the behavior of this type of dampers is known as the phenomenological model, which was proposed by Spencer Jr. *et al.* (1997). This model works based on a modified hysteresis Bouc-Wen model. The force f generated by the MR damper is calculated using Equation (1):

$$f = \alpha z + c_0\left(\dot{x}-\dot{y}\right)+k_0\left(x-y\right)+k_1\left(x-x_0\right) \quad (1)$$

where z is the evolutionary variable of the Bouc-Wen model that is calculated through Equation (2):

$$z = -\gamma\left|\dot{x}-\dot{y}\right|\left|z\right|\left|z\right|^{n-1} - \beta\left(\dot{x}-\dot{y}\right)\left|z\right|^{n} + A\left(\dot{x}-\dot{y}\right) \quad (2)$$

$$\dot{y} = \frac{1}{\left(c_0+c_1\right)}\left[\alpha z + c_0\dot{x} + k_0\left(x-y\right)\right] \quad (3)$$

In the above Equations, the parameters γ, β, and A are constant setting parameters; k_1 is the stiffness of the MR damper; c_0 is the viscous damping observed at higher velocities; c_1 is the damping coefficient of the device; k_0 x_0 is a parameter to control stiffness at high velocities; and x_0 is the initial displacement of the device associated with nominal damper force due to accumulation.

The general properties of these devices can be seen in Table 1. The parameters that describe the behavior of the dampers are defined by Basili (2006).

Table 1. Properties of the MR damper used

General Properties	Values
Compressed length (mm)	155
Extended length (mm)	208
Body diameter (mm)	41,4
Damper forces (N)	22 240
Operating temperature (°C)	Max 71
Input voltage (V)	12 DC
Response time (ms)	< 15

Source: Authors

Proposed structural control

The proposed structural control works based on a fuzzy-logic algorithm that manages the control forces generated by the MR dampers. This algorithm uses heuristic knowledge obtained from the real data of the structural systems studied in order to produce an optimal control action through a set of functions and classification parameters. The algorithm produces the optimal control action by introducing variable forces over time from the manipulation of the voltage to be induced in the MR dampers. An outline of the control project proposed for this work can be seen in Figure 2.

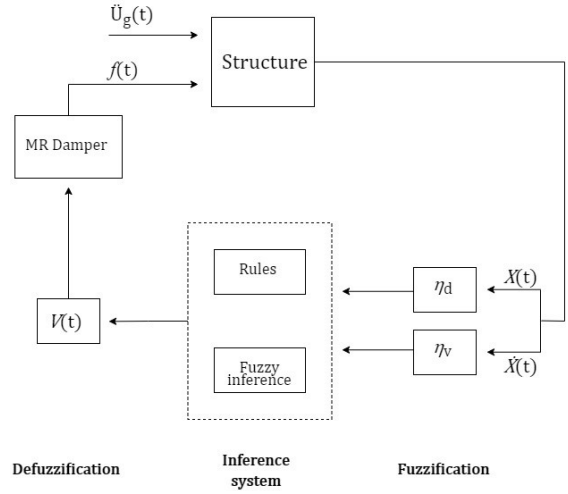

Figure 2. Structural control based on fuzzy-logic
Source: Authors

The controller uses the displacement $x(t)$ and velocitiy $\dot{x}(t)$ response functions of the building's first story. These variables must be normalized through a set of linear functions, since the range of study in the fuzzy universe is defined by the interval [-1, 1]. The normalization functions and scaling factors used in this work correspond to those defined by Liu *et al*. (2001) and Wilson (2005). Equations (4) and (5) describe the normalization functions for the displacement (η_d) and the velocity (η_v), respectively.

$$\eta_d = k_d \cdot x \tag{4}$$

$$\eta_v = k_v \cdot \dot{x} \tag{5}$$

where k_d is the displacement scaling factor, and k_v is the velocity scaling factor, both defined by Liu *et al*. (2001). Moreover, η_d and η_v are the first story values of displacement and velocity, respectively.

The controller's single output parameter is the voltage required by the MR damper to generate the optimal structural control forces. The output value of this variable is defined in the universe [0, 1], and it is defuzzified using the centroid method. The scaling factor that was used to determine the output voltage *V* in the real universe is described by Equation (6):

$$V = V_{max}\left(\frac{5}{3}s - \frac{1}{3}\right) \tag{6}$$

where V_{max} is the maximum voltage that can be provided to the MR damper, and s is the numerical output value obtained during defuzzification.

The input and output membership functions used in the fuzzification and defuzzification processes are composed of identical triangles with a 50% overlap. Figure 3 presents the input membership functions (displacement or velocity), whereas Figure 4 presents the output membership functions (voltage).

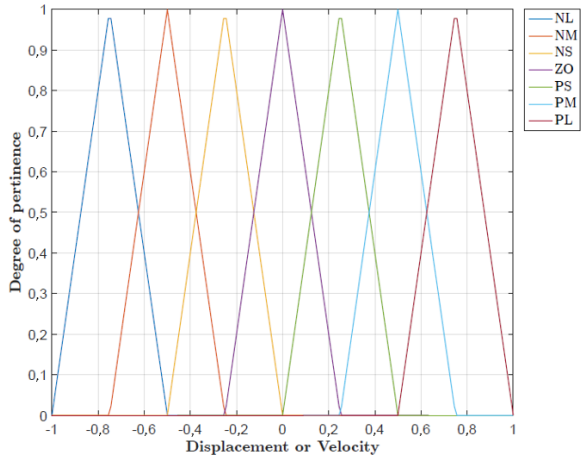

Figure 3. Input membership functions used in the fuzzification process
Source: Authors

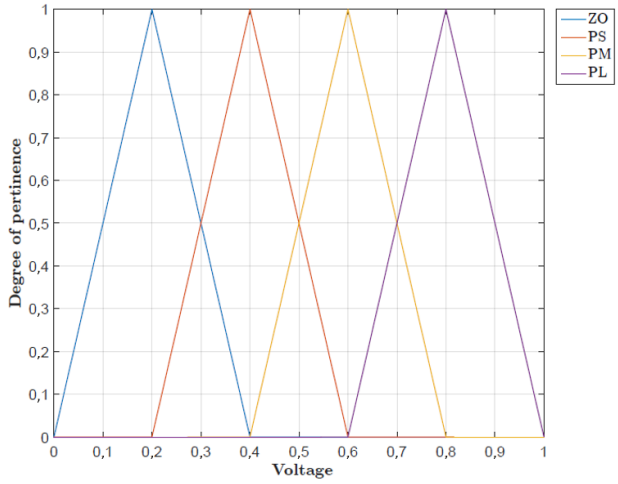

Figure 4. Output membership functions used in the defuzzification process
Source: Authors

Table 2 shows the controller inference system defined by Liu *et al*. (2001). The linguistic fuzzy values NL, NM, NS, ZO, PS, PM, and PL mean Negative Large, Negative Medium, Negative Small, Zero, Positive Small, Positive Medium, and Positive Large, respectively.

Table 2. Fuzzy inference system

$X(t)$ \ $\dot{X}(t)$	NG	NM	NP	ZO	PP	PM	PG
NG	PG	PG	PG	PM	ZO	ZO	ZO
NM	PG	PG	PG	PP	ZO	ZO	PP
NP	PG	PG	PG	ZO	ZO	PP	PM
ZO	PG	PM	PP	ZO	PP	PM	PG
PP	PM	PP	ZO	ZO	PG	PG	PG
PM	PP	ZO	ZO	PP	PG	PG	PG
PG	ZO	ZO	ZO	PM	PG	PG	PG

Source: Authors

The generation of optimal voltages, which allow the injection of damping forces with the capacity to dissipate a significant amount of energy caused by the ground motions, depends exclusively on the displacements and velocities of the first floor in each model. To adjust these parameters to the proposed set of fuzzy linguistic values, linear functions are used to normalize the responses of the structures in the universe of the defined pertinence functions.

The structural control implementation and the numerical simulations carried out to verify the performance of the controlled and uncontrolled frames were executed in the programming and numeric computing platform Matlab.

Results and discussion

As mentioned above, each model, in its uncontrolled and controlled configuration, was excited by four different seismic records, and their respective numerical responses

were determined. Every controlled structure was equipped with two MR dampers installed in the two first stories of the frames. The MR dampers were managed by the classic fuzzy-logic algorithm described above, which calculates the optimal damping forces to be provided by the MR dampers in order to reduce the structural response. A comparative response analysis for the controlled and uncontrolled systems was carried out to evaluate the performance of the developed controller.

Figure 5 shows the behavior of the absolute maximum displacement of each story for all the studied structures, considering the uncontrolled and controlled configurations. In this graph, the first, second, and third columns represent the maximum lateral displacement of each floor for models A, B, and C, respectively, when the structures are subjected to the El Centro, Christchurch-Lyttelton, Mistrato, and Algarrobo ground motions.

The greatest reductions in the peak displacements always occur in the two highest stories of the structures. It is also possible to affirm that the use of the fuzzy-logic-based controllers in the different models does not ensure a uniform trend in the lateral displacement reduction for all the stories of the structural systems. For instance, in model A, it is possible to get reductions of up to 78% in the lateral displacement of each story of the structure when it is subjected to the ground acceleration caused by El Centro

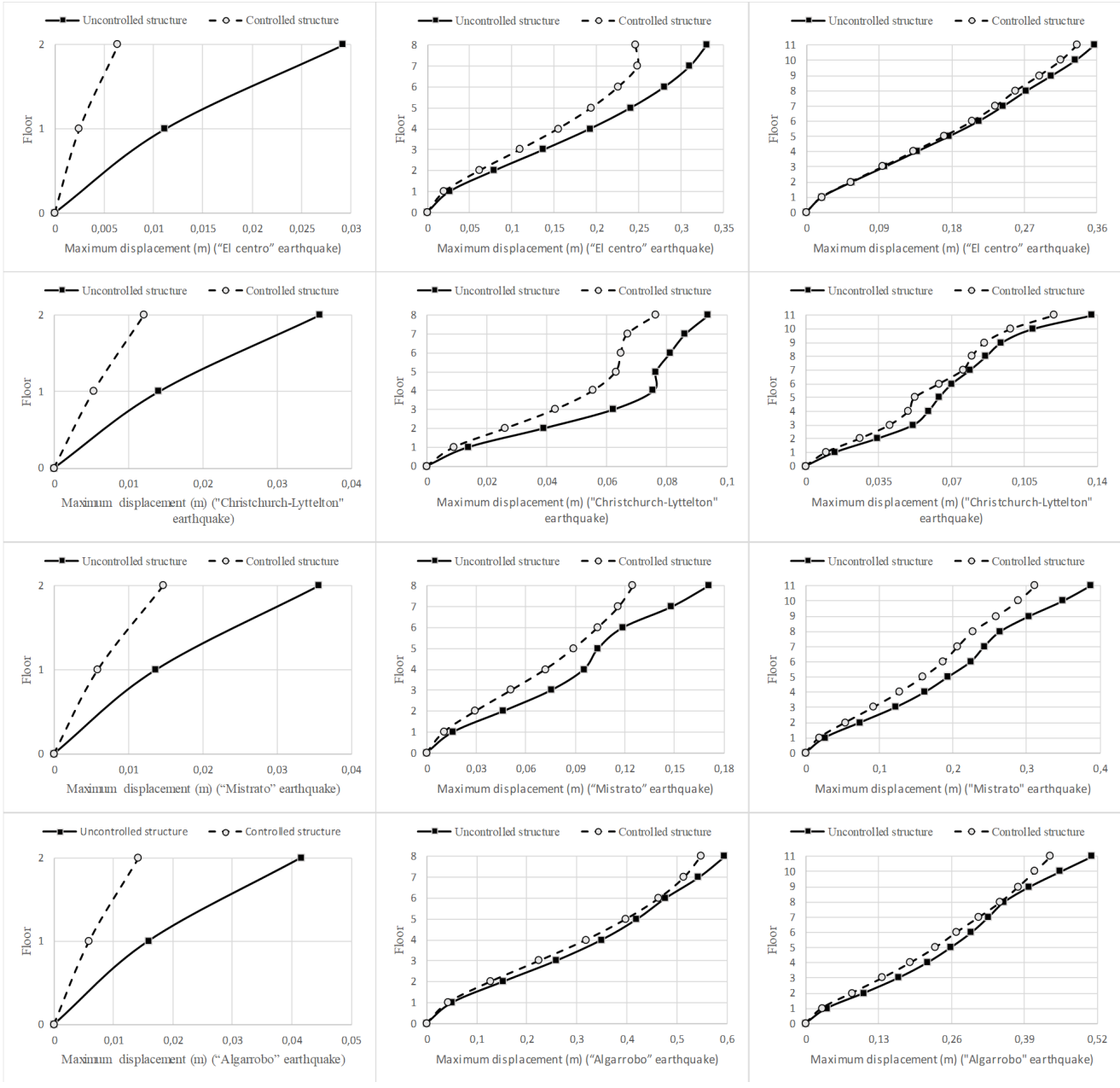

Figure 5. Absolute maximum displacements for the uncontrolled and controlled structures
Source: Authors

earthquake. On the other side, the reductions of the lateral displacements of each floor of model A when it is subjected to the Mistrato ground motion are up to 62%.

The analysis of the reduction of the lateral displacements of models B and C have some characteristics that can be generalized and allow inferring some interesting aspects about the performance of the controller used. First, the structures in models B and C are 4 and 5,5 times higher, respectively, than the structure discretized in the model A, so the lateral displacements of models B and C have higher displacement magnitudes. In spite of this, it is possible to see that the percentages of lateral displacement reduction for the controlled structures with eight and eleven levels are lower than those corresponding to model A, thus obtaining maximum reduction percentages of up to 27% in model B and up to 20% in model C.

Although the decrease in the reduction percentages may lead to consider that the configuration used in the controller loses its effectiveness in high structures, a deeper analysis allows deducing that the reduction in the lateral displacement magnitudes of the structures in models B and C are similar or even higher than those obtained for model A. An example of this is the response of the three modeled structures when excited by the acceleration produced by the Algarrobo earthquake. For this case, a maximum lateral displacement reduction of 2,78 cm was reached on the second floor of model A. On the other hand, the magnitude of the maximum lateral displacement reductions for the discretized structures in models B and C reached values of 6,57 and 7,54 cm on floors eight and eleven, respectively. These results reaffirm that the control system is a valid strategy to be used in the reduction of lateral displacement in low- and medium-height buildings.

The Algarrobo ground motion caused the maximum responses in the uncontrolled models among all the studied cases. As expected, these maximum responses took place at the top story of each structure. In model A, the maximum lateral displacement, velocity, and acceleration were 0,0416 m, 1,46 m/s, and 55,12 m/s^2, respectively. The control system's operation reduces these response parameters to 0,0138 m, 0,54 m/s, and 30,04 m/s^2, implying reductions of 66,83, 63,01, and 45,50%, respectively.

For the uncontrolled models B and C, the maximum lateral displacement at the top story was 0,5952 and 0,5104 m, respectively. The same parameters for the controlled configurations of models B and C were 0,5295 and 0,4350 m, which represents response decreases of 11,04 and 14,77%. It is remarkable that the maximum displacement of model B is larger than that of model C. The main reason for this is that model C, despite being taller, is stiffer than the idealized structure in model B. Likewise, the maximum velocity of models B and C were 5,28 and 5,87 m/s for the uncontrolled configurations and 4,39 and 4,42 m/s for the controlled configurations, thus consolidating velocity parameter reductions of 16,86% for model B and 24,70% for model C. The peak accelerations for the uncontrolled models B and C were 62,81 and 97,94 m/s^2, respectively. These values drop to 57,18 and 56,60 m/s^2 when the MR damper-based control system is installed on the structures. The achieved acceleration reductions were 8,96 and 42,21% for models B and C, respectively.

Table 3 presents a summary with the maximum lateral displacement values and RMS (Root Mean Square) values for the displacements of the uncontrolled and controlled structures for all the ground motions used. This Table also shows the corresponding percentages of the response reductions achieved in the controlled structures.

It is interesting to note the general behavior of the RMS displacement response in the studied structures. According to the results, the semi-active controller was able to reduce the RMS displacement values for the first and second stories of the discretized structure in case A by up to 96%. On the other hand, when the structure was subjected to the Mistrato earthquake, the smallest reductions in the RMS displacement response was evidenced, namely 34 and 38% for the first and second floor, respectively. The variation in the lateral displacement on the top story of model A when El Centro and Mistrato earthquakes excite the structure is shown in Figures 6 and 7, respectively.

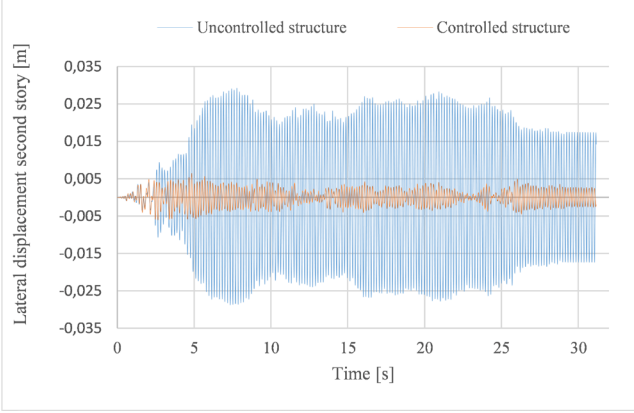

Figure 6. Displacement of the second floor of model A when the structure is subjected to El Centro ground motion record
Source: Authors

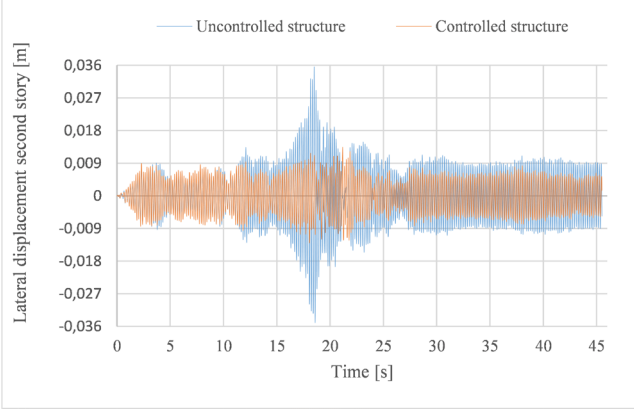

Figure 7. Displacement of the second floor of model A when the structure is subjected to the Mistrato ground motion record.
Source: Authors

Table 3. Summary of the response for the analyzed uncontrolled and controlled structures

	Model A															
	El Centro, 1940				Christchurch-Lyttelton, 2011				Mistrato, 1979				Algarrobo, 1985			
	Maximum displacement (m)		*RMS* value of displacement (m)		Maximum displacement (m)		*RMS* value of displacement (m)		Maximum displacement (m)		*RMS* value of displacement (m)		Maximum displacement (m)		*RMS* value of displacement (m)	
	1st Story	2nd Story	1st Story	2nd Story	1st Story	2nd Story	1st Story	2nd Story	1st Story	2nd Story	1st Story	2nd Story	1st Story	2nd Story	1st Story	2nd Story
Uncontrolled structure	0,0112	0,0292	0,0059	0,0154	0,0141	0,0357	0,0065	0,0170	0,0137	0,0356	0,0029	0,0076	0,0159	0,0416	0,0043	0,0112
Controlled structure	0,0026	0,0065	0,0008	0,0021	0,0057	0,0128	0,0014	0,0035	0,0056	0,0135	0,0019	0,0047	0,0057	0,0138	0,0021	0,0054
Reduction (%)	76,79	77,74	86,44	86,36	59,57	64,15	78,46	79,41	59,12	62,08	34,48	38,16	64,15	66,83	51,16	51,79
	Model B															
	El Centro, 1940				Christchurch-Lyttelton, 2011				Mistrato, 1979				Algarrobo, 1985			
	Maximum displacement (m)		*RMS* value of displacement (m)		Maximum displacement (m)		*RMS* value of displacement (m)		Maximum displacement (m)		*RMS* value of displacement (m)		Maximum displacement (m)		*RMS* value of displacement (m)	
	7th Story	8th Story	7th Story	8th Story	7th Story	8th Story	7th Story	8th Story	7th Story	8th Story	7th Story	8th Story	7th Story	8th Story	7th Story	8th Story
Uncontrolled structure	0,3102	0,3301	0,1733	0,1848	0,0739	0,0937	0,0288	0,0350	0,1482	0,1706	0,0469	0,0518	0,5433	0,5952	0,2352	0,2513
Controlled structure	0,2470	0,2624	0,1269	0,1353	0,0663	0,0756	0,0237	0,0256	0,1155	0,1244	0,0405	0,0436	0,4984	0,5295	0,2118	0,2260
Reduction (%)	20,37	20,51	26,77	26,79	10,28	19,32	17,71	26,86	22,06	27,08	13,65	15,83	8,26	11,04	9,95	10,07
	Model C															
	El Centro, 1940				Christchurch-Lyttelton, 2011				Mistrato, 1979				Algarrobo, 1985			
	Maximum displacement (m)		*RMS* value of displacement (m)		Maximum displacement (m)		*RMS* value of displacement (m)		Maximum displacement (m)		*RMS* value of displacement (m)		Maximum displacement (m)		*RMS* value of displacement (m)	
	10th Story	11th Story	10th Story	11th Story	10th Story	11th Story	10th Story	11th Story	10th Story	11th Story	10th Story	11th Story	10th Story	11th Story	10th Story	11th Story
Uncontrolled structure	0,3334	0,3567	0,1704	0,1794	0,1089	0,1375	0,0347	0,0442	0,3490	0,3867	0,1247	0,1335	0,4538	0,5104	0,1676	0,1783
Controlled structure	0,3140	0,3346	0,1590	0,1672	0,0993	0,1195	0,0250	0,0289	0,2882	0,3110	0,1118	0,1187	0,4062	0,4350	0,1488	0,1572
Reduction (%)	5,82	6,20	6,69	6,80	8,82	13,09	27,95	34,62	17,42	19,58	10,34	11,09	10,49	14,77	11,22	11,83

Source: Authors

The data obtained from the analysis of the RMS displacement response for models B and C ratify the reductions obtained using the developed controller. In model B, the highest reduction of the RMS displacement response for the controlled structure was reached when the structure was excited by El Centro earthquake, obtaining reductions of up to 27% for the last two stories of the building. On the other hand, when the Algarrobo earthquake excited the structure, the RMS displacement responses were lower, with decreased up to 10% in the last two stories of the modeled building. The reduction in the RMS values of displacement in the last two stories of the controlled model C was up to 34%. This occurred when the structure was excited by the ground motion record of Christchurch-Lyttelton. On the contrary, the lower performance of the controlled model C occurred when it was subjected to the acceleration record of El Centro earthquake, in which the reduction in the RMS value of displacement was around 7%. Figures 8 and 9 present the last story's time histories of models B and C in their uncontrolled and controlled configurations for the El Centro and Christchurch-Lyttelton records, respectively. These figures clearly show the performance of the controller based on MR dampers acting to reduce the lateral displacement of the last story of the structure.

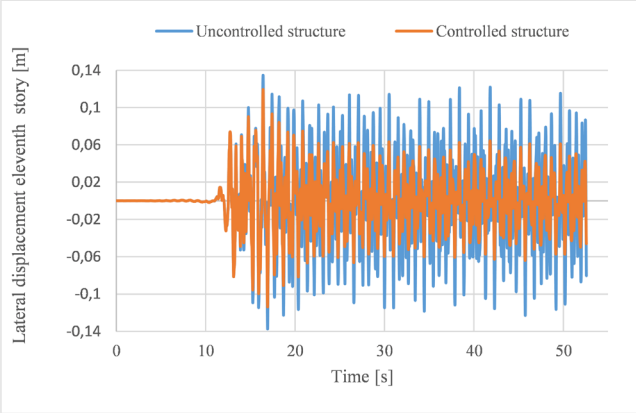

Figure 8. Displacement of the eight floor of model B when the structure is subjected to El Centro ground motion record
Source: Authors

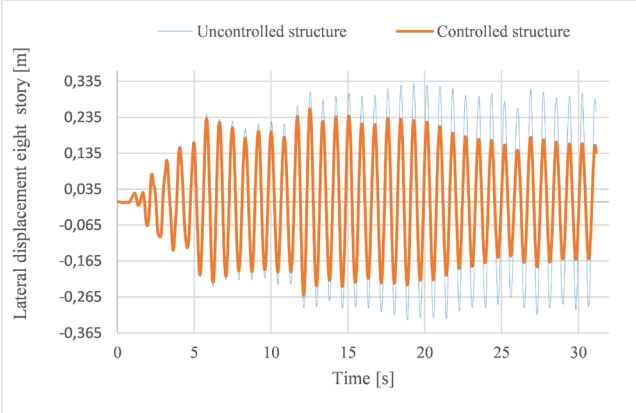

Figure 9. Displacement of the eleventh floor of model C when the structure is subjected to the Christchurch-Lyttelton ground motion record
Source: Authors

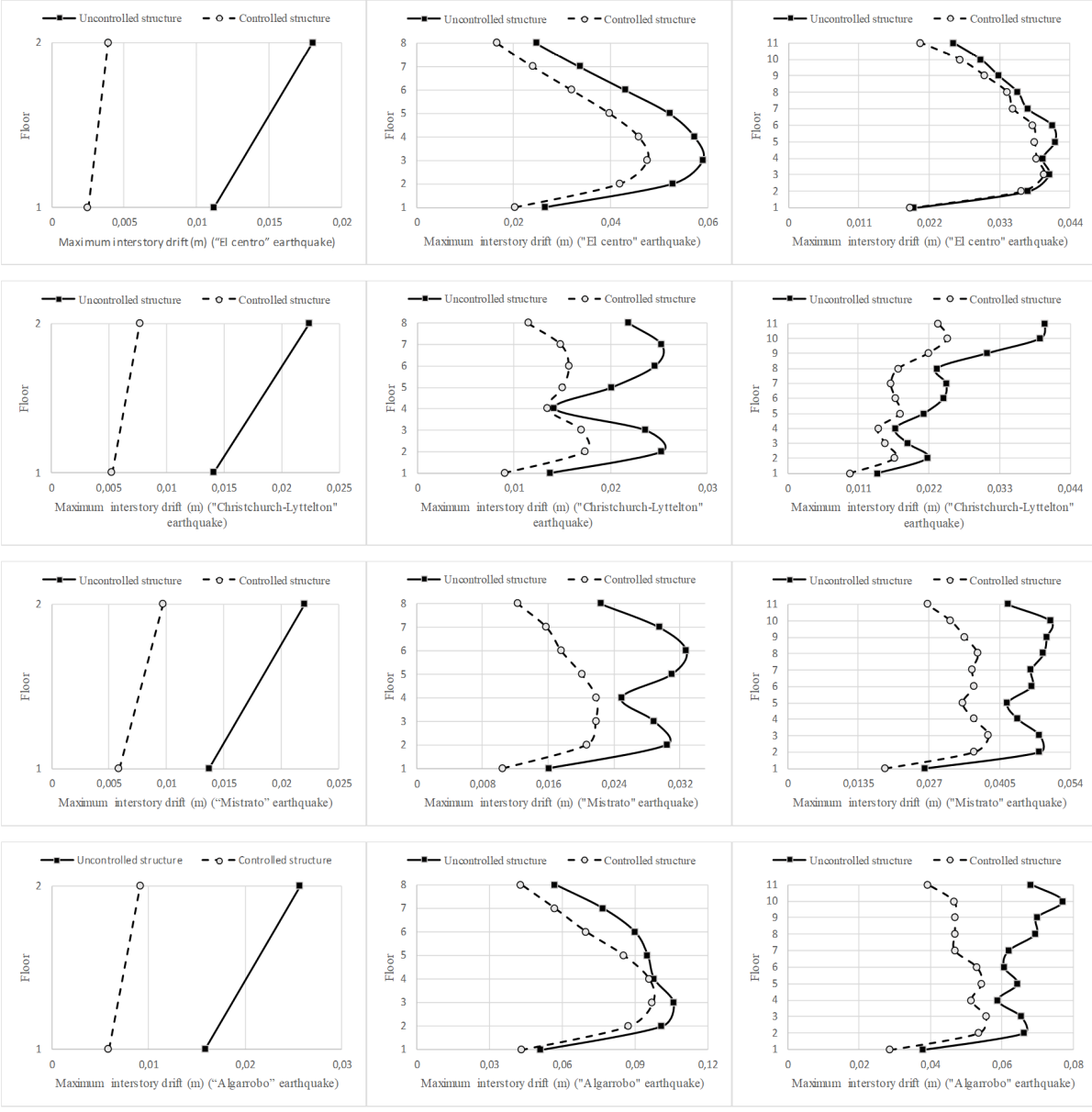

Figure 10. Interstory drift graphs for the uncontrolled and controlled structures
Source: Authors

Figure 10 presents the graphs of the maximum relative lateral displacements between consecutive floors of the three buildings in their controlled and uncontrolled configurations. Based on the analysis of this Figure, it is possible to demonstrate the effect of drift reduction in the controlled structures. For instance, in the study of models A and C, higher reductions were observed on the drifts of the last floors of the structures. Maximum horizontal interstory displacements of up to 1,65 cm (64,20% equivalent reduction) and up to 2,89 cm (42,31% equivalent reduction) were obtained for models A and C, respectively. On the other hand, in model B, the highest drift decrease was obtained for the middle stories of the building, with the sixth story generally being the level where the highest reductions were found, obtaining reduction values of up to 2,01 cm (equivalent reduction of 22,33%). All these reductions were reached when the excitation affecting the structures was the Algarrobo earthquake.

There is another important result, which is obtained by analyzing the story drifts graphs: all the inter-story drifts showed improvements with the control system proposed in this work. This means, that the control device works adequately in reducing the structure's interstory drifts, thus decreasing the magnitude of this parameter in the three models, regardless of the height of the next considered story. In addition, these data confirm that there are effective reductions in the lateral displacements of all the stories of the structures studied when using the controller based on MR dampers.

Conclusions

This study investigated the implementation of an MR damper-based control system to reduce the structural response in three different plane frame buildings subjected to diverse soil accelerations. An algorithm based on fuzzy logic was used to calculate the voltage required by the MR damper to generate the optimal damping forces, depending on the input parameters of displacement and the velocity of the first floor of the structures. Based on the numerical results obtained, it is concluded that the semi-active controller based on the set of MR dampers and the fuzzy logic control algorithm is an effective tool to reduce the lateral displacements of framed low- and medium-height buildings. The performance obtained in the three controlled models shows reductions for the lateral displacement of up to 78, 27, and 20%, as well as reduction percentages of the interstory drift of up to 78, 47, and 42% for models A, B, and C, respectively. Furthermore, the estimation of the evolution of the horizontal displacements over time in terms of the RMS values demonstrates the success of the controller system in achieving reductions of up to 86% for both floors of model A. In the case of models B and C, reduction rates for the RMS value of displacement of up to 26 and 34% were determined for the last levels of the buildings. Thus, the effectiveness of the developed controller was demonstrated, which opens the way for future efforts in the actual implementation of this type of technology, as well as in the optimization of MR damper configurations to make them more efficient.

Acknowledgements

The authors are grateful for the support provided by Universidad Nacional de Colombia, Medellín branch, in the development of this work.

References

Amini, F., Mohajeri, S. A., and Javanbakht, M. (2015). Semi-active control of isolated and damaged structures using online damage detection. *Smart Materials and Structures*, *24*(10), 105002. https://doi.org/10.1088/0964-1726/24/10/105002

Arzeytoon, A., Golafshani, A. A., Toufigh, V., and Mohammadi, H. (2017). Seismic performance of ribbed bracing system in passive control of structures. *Journal of Vibration and Control*, *23*(18), 2926-2941. https://doi.org/10.1177/1077546315623876

Basili, M., and de Angelis, M. (2007). Optimal passive control of adjacent structures interconnected with nonlinear hysteretic devices. *Journal of Sound and Vibration*, *301*(1), 106-125. https://doi.org/10.1016/j.jsv.2006.09.027

Bathaei, A., Zahrai, S. M., and Ramezani, M. (2018). Semi-active seismic control of an 11-DOF building model with TMD+MR damper using type-1 and -2 fuzzy algorithms. *Journal of Vibration and Control*, *24*(13), 2938-2953. https://doi.org/10.1177/1077546317696369

Behrooz, M., Wang, X., and Gordaninejad, F. (2014). Modeling of a new semi-active/passive magnetorheological elastomer isolator. *Smart Materials and Structures*, *23*(4), 45013. https://doi.org/10.1088/0964-1726/23/4/045013

Bitaraf, M., Hurlebaus, S., and Barroso, L. R. (2012). Active and semi-active adaptive control for undamaged and damaged building structures under seismic load. *Computer-Aided Civil and Infrastructure Engineering*, *27*(1), 48-64. https://doi.org/10.1111/j.1467-8667.2011.00719.x

Cha, Y.-J., and Agrawal, A. K. (2017). Seismic retrofit of MRF buildings using decentralized semi-active control for multi-target performances. *Earthquake Engineering and Structural Dynamics*, *46*(3), 409-424. https://doi.org/10.1002/eqe.2796

Chowdhury, S., Banerjee, A., and Adhikari, S. (2021). Enhanced seismic base isolation using inertial amplifiers. *Structures*, *33*, 1340-1353. https://doi.org/10.1016/j.istruc.2021.04.089

Constantinou, M. C. (1994).Passive energy dissipation development in U.S. In M.C. Constantinou (Ed.), *Passive and Active Structural Vibration Control in Civil Engineering* (pp. 255-269). Springer. https://doi.org/10.1007/978-3-7091-3012-4

Cruze, D., Hemalatha, G., Magdalene, A., Tensing, D., and Sundar Manoharan, S. (2018). Magnetorheological damper for performance enhancement against seismic forces. In H. Rodrigues, A. Elnashai, and G. M. Calvi (Eds.), *Facing the Challenges in Structural Engineering* (pp. 104-117). Springer International Publishing.

Cruze, D., Hemalatha, G., Noroozinejad, F. E., Arnab, B., Sarala, L., and Manoharan, S. S. (2021). Seismic performance evaluation of a recently developed magnetorheological damper: experimental investigation. *Practice Periodical on Structural Design and Construction*, *26*(1), 4020061. https://doi.org/10.1061/(ASCE)SC.1943-5576.0000544

Downey, A., Cao, L., Laflamme, S., Taylor, D., and Ricles, J. (2016). High capacity variable friction damper based on band brake technology. *Engineering Structures*, *113*, 287-298. https://doi.org/10.1016/j.engstruct.2016.01.035

Gutiérrez, M. R., and Navarro, G. S. (2013). Control activo de vibraciones en estructuras tipo edificio usando actuadores piezoeléctricos y retroalimentación positiva de la aceleración. *Dyna*, *80*(179), 116-125. https://repositorio.unal.edu.co/handle/unal/41449

Housner, G. W., Bergman, L. A., Caughey, T. K., Chassiakos, A. G., Claus, R. O., Masri, S. F., Skelton, R. E., Soong, T. T., Spencer, B. F., and Yao, J. T. P. (1997). Structural control: Past, present, and future. *Journal of Engineering Mechanics*, *123*(9), 897-971. https://doi.org/10.1061/(ASCE)0733-9399(1997)123:9(897)

K-Karamodin, A., and H-Kazemi, H. (2010). Semi-active control of structures using neuro-predictive algorithm for MR dampers. *Structural Control and Health Monitoring*, *17*(3), 237-253. https://doi.org/10.1002/stc.278

Kannan, S., Uras, H. M., and Aktan, H. M. (1995). Active control of building seismic response by energy dissipation. *Earthquake Engineering and Structural Dynamics*, *24*(5), 747-759. https://doi.org/10.1002/eqe.4290240510

Kataria, N. P., and Jangid, R. S. (2016). Seismic protection of the horizontally curved bridge with semi-active variable stiffness damper and isolation system. *Advances in Structural Engineering*, *19*(7), 1103-1117. https://doi.org/10.1177/1369433216634477

Kaveh, A., Javadi, S. M., and Moghanni, R. M. (2020). Optimal structural control of tall buildings using tuned mass dampers via chaotic optimization algorithm. *Structures*, *28*, 2704-2713. https://doi.org/10.1016/j.istruc.2020.11.002

Khodabandolehlou, H., Pekcan, G., Fadali, M. S., and Salem, M. M. A. (2018). Active neural predictive control of seismically isolated structures. *Structural Control and Health Monitoring*, *25*(1), e2061. https://doi.org/10.1002/stc.2061

Kim, H., and Adeli, H. (2005). Hybrid control of irregular steel highrise building structures under seismic excitations. *International Journal for Numerical Methods in Engineering*, *63*, 1757-1774. https://doi.org/10.1002/nme.1336

Kori, J. G., and Jangid, R. S. (2008). Semiactive control of seismically isolated bridges. *International Journal of Structural Stability and Dynamics*, *08*(04), 547-568. https://doi.org/10.1142/S021945540800279X

Lara-Valencia, L. A., Farbiarz-Farbiarz, Y., and Valencia-González, Y. (2020). Design of a tuned mass damper inerter (tmdi) based on an exhaustive search optimization for structural control of buildings under seismic excitations. *Shock and Vibration*, *2020,* 8875268. https://doi.org/10.1155/2020/8875268

Lara-Valencia, L. A., Valencia-González, Y., and de Brito, J. L. V. (2015). Use of fuzzy logic for the administration of a structural control system based on magnetorheological dampers. *Revista Facultad de Ingeniería*, *74*(1), 151-164. https://revistas.udea.edu.co/index.php/ingenieria/article/view/16461?articlesBySimilarityPage=71

Lara-Valencia, L. A. (2011). *Estudo de algorítimo de controle semi-ativo aplicados a amortecedores* [Doctoral thesis, Universidade de Brasilia]. https://repositorio.unb.br/handle/10482/9389

Liu, Y., Gordaninejad, F., Evrensel, C. A., and Hitchcock, G. H. (2001, July 30). *Experimental study on fuzzy logic vibration control of a bridge using fail-safe magnetorheological fluid dampers* [Conference presentation]. SPIE's 8th Annual International Symposium on Smart Structures and Materials, Newport beach, CA, USA. https://doi.org/10.1117/12.434135

Lord Company (2006). *Products and solutions*. https://www.lord.com/products-and-solutions

Madhekar, S. N., and Jangid, R. S. (2009). Variable dampers for earthquake protection of benchmark highway bridges. *Smart Materials and Structures*, *18*(11), 115011. https://doi.org/10.1088/0964-1726/18/11/115011

Mohammadi, R. K., Ghamari, H., and Farsangi, E. N. (2021). Active control of building structures under seismic load using a new uniform deformation-based control algorithm. *Structures*, *33*, 593-605. https://doi.org/10.1016/j.istruc.2021.04.054

Omidi, E., and Mahmoodi, N. (2015). Hybrid positive feedback control for active vibration attenuation of flexible structures. *IEEE/ASME Transactions on Mechatronics*, *20*(4), 1790-1797. https://doi.org/10.1109/TMECH.2014.2354599

Pahlavan, L., and Rezaeepazhand, J. (2007). Dynamic response analysis and vibration control of a cantilever beam with a squeeze-mode electrorheological damper. *Smart Materials and Structures*, *16*(6), 2183-2189. https://doi.org/10.1088/0964-1726/16/6/021

Pourzeynali, S., Lavasani, H. H., and Modarayi, A. H. (2007). Active control of high rise building structures using fuzzy logic and genetic algorithms. *Engineering Structures*, *29*(3), 346-357. https://doi.org/10.1016/j.engstruct.2006.04.015

Selmani, F. H. (2020, October 31). Passive control of structures – The dynamic case. *UBT International Conference, 239*, 165-174. https://doi.org/10.33107/ubt-ic.2020.82

Shih, M.-H., and Sung, W.-P. (2021). Structural control effect and performance of structure under control of impulse semi-active mass control mechanism. *Iranian Journal of Science and Technology, Transactions of Civil Engineering*, *45*(2), 1211-1226. https://doi.org/10.1007/s40996-020-00387-9

Singh, M. P., Matheu, E. E., and Suárez, L. E. (1997). Active and semi-active control of structures under seismic excitation. *Earthquake Engineering and Structural Dynamics*, *26*(2), 193-213. https://doi.org/10.1002/(SICI)1096-9845(199702)26:2%3C193::AID-EQE634%3E3.0.CO;2-%23

Smanchai, S., and Yao, J. (1978). Active control of building structures. Journal of the engineer-ing mechanics division. *Journal of the Engineering Mechanics Division, 104*(2), 335-350. https://doi.org/10.1061/JMCEA3.0002335

Spencer Jr, B., Dyke, S. J., Sain, M. K., and Carlson, J. D. (1997). Phenomenological model for magnetorheological dampers. *Journal of Engineering Mechanics*, *123*(3), 230-238. https://doi.org/10.1061/(ASCE)0733-9399(1997)123:3(230)

Subramaniam, R. S., Reinhorn, A. M., Riley, M. A., and Nagarajaiah, S. (1996). Hybrid control of structures using fuzzy logic. *Computer-Aided Civil and Infrastructure Engineering*, *11*(1), 1-17. https://doi.org/10.1111/j.1467-8667.1996.tb00305.x

Sun, C., and Nagarajaiah, S. (2014). Study on semi-active tuned mass damper with variable damping and stiffness under seismic excitations. *Structural Control and Health Monitoring*, *21*(6), 890-906. https://doi.org/10.1002/stc.1620

Taniguchi, M., Fujita, K., Tsuji, M., and Takewaki, I. (2016). Hybrid control system for greater resilience using multiple isolation and building connection. *Frontiers in Built Environment*, *2,* 26. https://doi.org/10.3389/fbuil.2016.00026

Wilson, C. M. D. (2005). *Fuzzy control of magnetorheological dampers for vibration reduction of seismically excited structures* [Doctoral thesis, The Florida State University].

Xu, Z.-D., Shen, Y.-P., and Guo, Y.-Q. (2003). Semi-active control of structures incorporated with magnetorheological dampers using neural networks. *Smart Materials and Structures*, *12*(1), 80-87. https://doi.org/10.1088/0964-1726/12/1/309

Yang, J. N., Li, Z., Danielians, A., and Liu, S. C. (1992). Aseismic hybrid control of nonlinear and hysteretic structures I. *Journal of Engineering Mechanics*, *118*(7), 1423-1440. https://doi.org/10.1061/(ASCE)0733-9399(1992)118:7(1423)

Zamani, A. A., Tavakoli, S., and Etedali, S. (2017). Control of piezoelectric friction dampers in smart base-isolated structures using self-tuning and adaptive fuzzy proportional-derivative controllers. *Journal of Intelligent Material Systems and Structures*, *28*(10), 1287-1302. https://doi.org/10.1177/1045389X16667561

Zhang, Z., and Balendra, T. (2013). Passive control of bilinear hysteretic structures by tuned mass damper for narrow band seismic motions. *Engineering Structures*, *54*, 103-111. https://doi.org/10.1016/j.engstruct.2013.03.044

Zhao, Z., Zhang, R., Wierschem, N. E., Jiang, Y., and Pan, C. (2020). Displacement mitigation–oriented design and mechanism for inerter-based isolation system. *Journal of Vibration and Control*, *27*(17-18), 1991-2003. https://doi.org/10.1177/1077546320951662

Zhou, Y., and Zheng, S. (2020). Machine-learning based hybrid demand-side controller for high-rise office buildings with high energy flexibilities. *Applied Energy*, *262*, 114416. https://doi.org/10.1016/j.apenergy.2019.114416